ELSEVIER

Psychophysical evidence for a radial motion bias in complex motion discrimination

Scott A. Beardsley [*], Lucia M. Vaina

Brain and Vision Research Laboratory, Department of Biomedical Engineering, Boston University, 44 Cummington Street, Boston, MA 02215, United States

Abstract

In a graded motion pattern task we measured observers' ability to discriminate small changes in the global direction of complex motion patterns. Performance varied systematically as a function of the test motion (radial, circular, or spiral) with thresholds for radial motions significantly lower than for circular motions. Thresholds for spiral motions were intermediate. In all cases thresholds were lower than for direction discrimination using planar motions and increased with removal of the radial speed gradient, consistent with the use of motion pattern specific mechanisms that integrate motion along complex trajectories. The radial motion bias and preference for speed gradients observed here is similar to the preference for expanding motions and speed gradients reported in cortical area MSTd, and may suggest the presence of comparable neural mechanisms in the human visual motion system.
© 2005 Elsevier Ltd. All rights reserved.

1. Introduction

Much of the research examining motion pattern processing in the human visual system has focused on an observer's ability to detect coherent motion in the presence of a masking background noise. A variety of masking conditions, including both random motion and conflicting motion patterns, and adaptation studies have been used to quantify the existence of motion pattern mechanisms in the visual motion pathway (Burr, Badcock, & Ross, 2001; Burr, Morrone, & Vaina, 1998; Freeman & Harris, 1992; Morrone, Burr, Di Pietro, & Stefanelli, 1999; Morrone, Burr, & Vaina, 1995; Snowden & Milne, 1996, 1997). The qualitative similarities between these mechanisms and motion pattern responsive cells in the dorsal medial superior temporal area (MSTd)

of non-human primates has lead to speculation that similar neural mechanisms may exist in the human visual system. This idea is supported by functional imaging studies of motion pattern processing that have reported significant activation in an area referred to as hMT, the human homologue of the MT/MST complex (Greenlee, 2000; Morrone et al., 2000; Tootell et al., 1995; Vaina, Solovyev, Kopcik, & Chowdhury, 2000); for a review see (Vaina & Soloviev, 2004).

If, as has been proposed, MSTd does play a role in motion pattern processing, one would expect to observe psychophysical correlates to the visual motion properties reported there and in other motion pattern responsive areas to which it projects (Anderson & Siegel, 1999; Duffy & Wurtz, 1991a; Geesaman & Andersen, 1996; Graziano, Anderson, & Snowden, 1994; Read & Siegel, 1997; Schaafsma & Duysens, 1996; Siegel & Read, 1997); for a review see (Raffi & Siegel, 2004). In particular, the continuous neural representation of spiral motions and systematic bias toward both

---
[*] Corresponding author. Tel.: +1 6173 537 344; fax: +1 6173 530 731.
  E-mail address: sbeardsl@bu.edu (S.A. Beardsley).

expanding motions and radial speed gradients would seem to be natural identifying characteristics that could be used to further link psychophysical and neural mechanisms.

Psychophysical studies of complex motion processing have consistently failed to observe such differences. Studies of motion pattern discrimination within masking motion noise have found no significant difference between radial and circular motions (Morrone et al., 1999). Similarly, detection thresholds for circular motion have been shown to be the same as, or even better than those for radial motion (Burr et al., 2001; Meese & Anderson, 2002; Morrone et al., 1999). By comparison, detection thresholds for spiral motions tend to be higher than for radial or circular motions (Morrone et al., 1999), leading to the suggestion that the human visual system contains a cardinal representation for wide-field motion patterns.

Masking and sub-threshold summation studies using orthogonal motions generally support this idea (Burr et al., 2001; Freeman & Harris, 1992; Te Pas, Kappers, & Koenderink, 1996), although the existence of less sensitive spiral motion mechanisms cannot be ruled out (Burr et al., 2001). Sub-threshold summation experiments using more similar motion pattern components suggest that this may in fact be the case. Together with a simple model comparing best fit psychophysical sensitivity using four (cardinal) versus eight (cardinal + spiral) motion mechanisms, Meese and Anderson (2002) showed that human performance was better accounted for by a cardinal + spiral model, although they noted that the sensitivity of the intermediate spiral mechanisms was typically lower. This agrees well with coherence detection experiments in which thresholds for radial, circular, and spiral motions are all similar (Burr et al., 2001; Meese & Anderson, 2002).

While the existence of spiral motion mechanisms is suggestive of a continuous motion pattern representation, the differences between neural and psychophysical mechanisms remain more striking than their similarities. The lack of psychophysical correlates to the expansion and speed gradient biases observed in cortex could be due to interspecies differences. Alternatively the detection of coarse direction differences in the motion coherence paradigm might not lend itself to direct comparison with motion pattern biases reported using fully coherent stimuli.

Here we present results from a novel psychophysical task designed to facilitate a more direct comparison between human performance and the reported visual motion properties in cortical areas, such as MSTd, believed to underlie complex motion processing (Anderson & Siegel, 1999; Duffy & Wurtz, 1991a; Geesaman & Andersen, 1996; Graziano et al., 1994; Schaafsma & Duysens, 1996; Siegel & Read, 1997). Using motion pattern stimuli similar to previous studies (Burr et al., 1998;

Freeman & Harris, 1992; Morrone et al., 1995) we have extended the basic direction discrimination task (Ball & Sekuler, 1979; De Bruyn & Orban, 1988; Watamaniuk, Sekuler, & Williams, 1989) to measure observers' sensitivity to small changes in the global direction of motion. We hypothesize that if MSTd-like mechanisms do play a role in human visual motion processing, then psychophysical performance on tasks designed to probe direction sensitivity within individual motion pattern mechanisms should result in measurable differences associated with the preferences for speed gradients and expanding motions reported in cortex.

2. General methods

2.1. Stimuli

Stimuli consisted of random dot kinematograms (RDKs) displayed on an AppleVision 1710 monitor in a 24° diameter annular region (central 4° removed). Each stimulus consisted of 190 uniformly distributed dots (4×4 pixels; 9.3 Cd/m^2) displayed on a low luminance (5.2 Cd/m^2) gray background. Movie sequences were generated off-line and displayed at 75 Hz in a calibrated gray-scale mode with 8-bit precision and a resolution of 832×624 pixels.

Stimuli were viewed binocularly at a distance of 54 cm and all stimulus apertures were *illusory* as defined by an absence of dots. At the subject viewing distance each dot subtended 9.8 min of visual angle and moved through a radial speed gradient whose maximum speed could be varied from 0.15 to 45 °/s ($0.125 * r$ to $3.75 * r$) between tests.

For an arbitrary motion pattern centered in the display, the displacement of a dot in polar co-ordinates (r, θ), was given by

$$\begin{pmatrix} \dot{r} \\ \dot{\theta} \end{pmatrix} = \omega \begin{pmatrix} r \cos \phi \\ \sin \phi \end{pmatrix} \qquad (1)$$

where r is the distance of the dot from the stimulus center, ϕ is the flow angle within a 2-D motion pattern space formed by combinations of radial and circular motion (Fig. 1) and ω is proportional to the dot speed. For each dot successive spatial positions were generated with floating-point precision by integrating the derivatives over the frame interval (Δt) and transforming the polar representation into the Cartesian co-ordinate system used by the display (Eq. (2)). The resulting system of equations provided a recursive calculation of the ith dot's floating-point position ($x_i(t + \Delta t)$, $y_i(t + \Delta t)$) relative to the stimulus center-of-motion that was based on the previous dot position ($x_i(t)$, $y_i(t)$), the user specified flow angle and dot speed. Dots were then displayed by rounding each dot's position to the nearest integer pixel location on the screen.
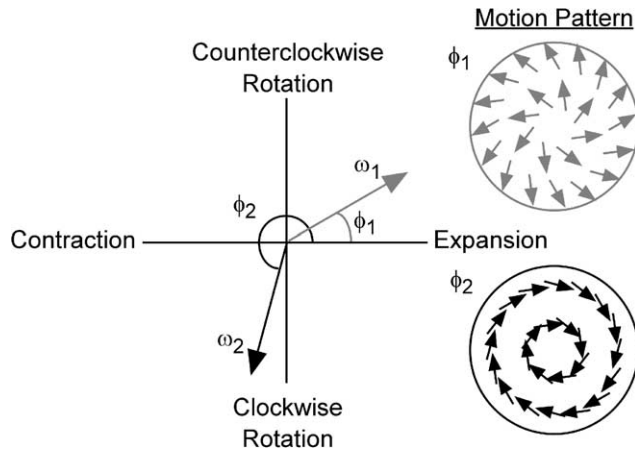
Fig. 1. Motion pattern space. Radial, circular, and spiral motions can be represented as vectors in a 2-D stimulus space where the flow angle (ϕ) defines the type of motion pattern relative to a 0° baseline expansion and the magnitude (ω) is proportional to the dot speed. Off-axis regions correspond to intermediate degrees of spiral motion.

$$\begin{pmatrix} x_{n+1} \\ y_{n+1} \end{pmatrix} = e^{\omega \cos \phi} \begin{pmatrix} x_n \cos(\omega \sin \phi) - y_n \sin(\omega \sin \phi) \\ x_n \sin(\omega \sin \phi) + y_n \cos(\omega \sin \phi) \end{pmatrix} \tag{2}$$

All stimuli were presented for 440 ms with a dot lifetime of 146 ms (11 frames). To minimize coherent stimulus flicker dots were replaced asynchronously by uniformly distributing the initial dot lifetimes among the first 11 frames. When dots exceeded their lifetime or moved beyond the stimulus boundaries they were assigned new positions and trajectories consistent with the specified motion pattern and the active maintenance of a constant density display (see Clifford, Beardsley, & Vaina, 1999 for details). Position-based discrimination cues associated with estimating the net spatial offset along dot trajectories was controlled by randomly perturbing the stimulus duration over the range ±40 ms, centered on the nominal stimulus duration (i.e., 440 ± 40 ms).

2.2. Experimental procedure

Prior to an experimental session, observers adapted to the background luminance of the display in a quiet darkened room. During the experiment, observers were required to maintain fixation on a small central square (11×11 pixels; 9.3 Cd/m^2) and pairs of motion patterns (500 ms interstimulus interval) were presented binocularly in a temporal two-alternative-forced-choice (2AFC) task using a constant stimulus design. For each observer and motion pattern, constant stimulus levels were specified relative to the average threshold (79% correct) obtained across three adaptive staircase sessions (~300–500 trials total). An auditory cue preceded each stimulus.

For each constant stimulus session, discrimination thresholds were calculated at the 82% correct level using

a weighted two-parameter Weibull fit to four constant stimulus levels (one observer, CC, was tested across six levels). A χ^2 goodness-of-fit measure with (v) degrees of freedom was used to exclude data sets with poor curve fits from further analysis ($\chi^2(v) > \chi_R^2(v)$; $p < 0.1$) (Bevington, 1969). For each experimental condition, performance was reported as the mean threshold ± 1 SE averaged across 8–15 constant stimulus sessions (~1000–1900 trials total) whose χ^2 measures fell below the rejection level (χ_R^2).

2.3. Observers

In total, six observers participated in the graded motion pattern (GMP) experiments. Four of the six were experienced psychophysical observers. Two observers (one experienced and one first-time psychophysical observer) also participated in the direction discrimination task. Four of the observers were naïve to the purpose of the study and all had 20/20 vision (2 corrected, 4 uncorrected). Prior to participation in the study written informed consent was obtained from all subjects in accordance with Boston University's Institutional Review Board Committee on research involving human subjects.

3. Experiment 1: Direction discrimination in radial and circular motions

In the first experiment we examined the ability of observers to discriminate small changes in the global direction of coherent radial and circular motions. If the visual system contains a uniform representation of equally sensitive motion pattern mechanisms then a simple pooling rule would predict direction discrimination to be the same for radial and circular motions (Beardsley & Vaina, 2001, 2004a, 2004b). The same would also be true for a cardinal representation of radial and circular motion mechanisms. In this context, motion pattern dependent changes in direction discrimination would suggest differences in the distribution and/or sensitivity of the underlying mechanisms.

In a control condition a subset of observers also performed a direction discrimination task containing translating dot motion. If the ability to discriminate changes in radial and circular direction is based on local direction mechanisms then we would predict that performance in the two tasks should be well matched.

3.1. Methods

3.1.1. Graded motion pattern (GMP) discrimination

In the GMP task, discrimination pairs of stimuli were formed by incrementing the flow angle (ϕ) of a test motion by ±ϕ_p in the 2-D motion pattern space (Fig. 2).
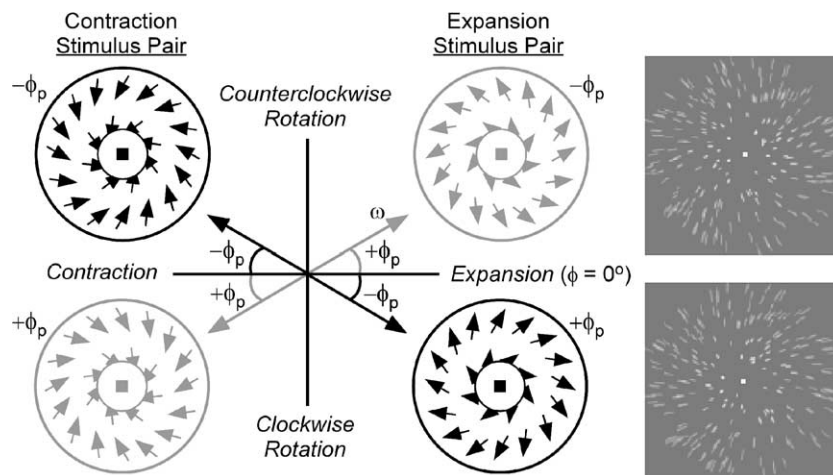
Fig. 2. Schematic representation of the graded motion pattern (GMP) task for radial motions. Stimuli were formed by changing the flow angle of the test motion (e.g., expansion or contraction) by $\pm\phi_p$. The images to the right illustrate time-lapsed versions of a stimulus pair for an expansion. For each stimulus pair observers were required to select the stimulus interval containing a clockwise change in the flow angle ($-\phi_p$) relative to the test motion (ϕ).

During each stimulus frame the change in flow angle corresponded to a rotation of each dot's trajectory by ϕ_p relative to the local direction of the test motion (Fig. 3). Computationally, this frame-wise change in trajectory was identical to the change in motion direction implemented in direction discrimination tests of simple translating motion (Ball & Sekuler, 1979; De Bruyn & Orban, 1988; Watamaniuk et al., 1989). However as
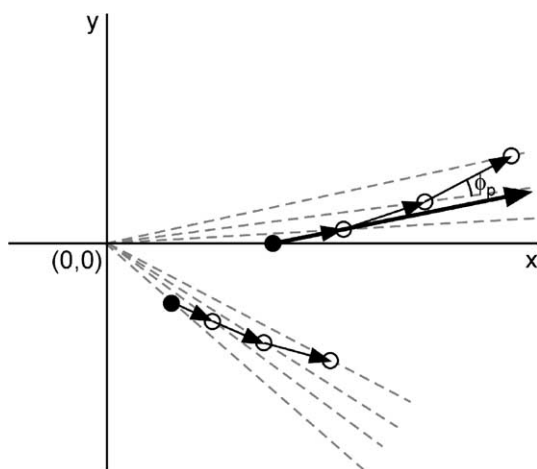
Fig. 3. Change in the local trajectory of a dot for an expanding test motion whose flow angle has been rotated counter-clockwise by ϕ_p. The change in flow angle was equivalent to rotating the dot's trajectory by ϕ_p relative to the local direction of the test motion (radial dashed lines) in each stimulus frame. Computationally, this frame-wise change in local motion direction was identical to the change in trajectory implemented in the direction discrimination task (thick arrow). In practice, the continuous change in direction with polar angle necessary to form each motion pattern meant that after a frame-wise displacement the local direction of the test motion was slightly different. This resulted in a cumulative change in net direction for motion pattern stimuli that was on average 7% greater over the lifetime of a dot with a maximum frame-wise deviation of 13% at the end of a dot's lifetime.

we discuss in Section 3.1.2, for the GMP task the net change in direction was slightly greater over the lifetime of a dot due to the systematic changes in local motion direction required to form complex motion patterns.

At the display resolution and subject viewing distance the minimum displacement of a dot between frames was approximately 2.5 s of arc. For small changes in flow angle the net change in direction across frames was probabilistic with a minimum detectable change of one-pixel over the lifetime of a dot. At the slower of the two mean dot speeds tested (8.4 °/s) this resulted in a minimum ϕ_p of 0.6–0.75° across the outer half of the stimulus aperture.[1] Careful observation of the stimulus for small changes in direction above this range ($\phi_p = 0.8°$) confirmed that the changes in direction appeared smooth and could be readily identified.

During a test session observers were presented with pairs of motion pattern stimuli shifted clockwise and counter-clockwise by ϕ_p. For each stimulus pair observers were required to press a key indicating the stimulus interval containing a clockwise change in flow angle ($\phi - \phi_p$) relative to the test motion. In practice the interpretation of motion pattern direction in terms of clockwise/counter-clockwise changes in flow angle was conceptually difficult. Observers' natural tendency was to perceive direction changes in terms of the addition of radial or circular motion components relative to the test motion. Except for a re-normalization of the dot speed following the change in flow angle, the two interpretations were functionally equivalent. As a result, during testing we utilized a conceptual simplification to the change in stimulus flow angle based on the addition of

---

[1] The radial speed gradient increases the minimum detectable ϕ_p with distance from stimulus center.

Table 1
Conceptual simplification of the clockwise change in flow angle judgment ($\phi - \phi_p$) for the GMP task

ϕ	Test motion	Conceptual simplification of $\phi - \phi_p$ discrimination
0	Expansion	Select stimulus interval containing CW motion
180	Contraction	
90	CCW rotation	Select stimulus interval containing expanding motion
270	CW rotation	
45	Exp-CCW spiral	Select stimulus interval containing more radial motion
225	Cont-CW spiral	
135	Cont-CCW spiral	Select stimulus interval containing more circular motion
315	Exp-CW spiral	

For each set of opposing test motions, observers were required to select the stimulus interval (first or second) containing the change in motion pattern direction indicated above. In cases where the simplified criteria mixed clockwise and counter-clockwise judgments within an interleaved pair of test motions (e.g., expansion and contraction) responses to test motions eliciting counter-clockwise judgments (e.g., contraction) were automatically inverted prior to analysis.

orthogonal radial (expansion/contraction) or circular (clockwise/counter-clockwise rotation) motion components (Table 1). For the radial and circular test motions tested in Experiment 1, observers were required to indicate the stimulus interval containing either a clockwise or expanding component of motion respectively.

Over the course of the experiment, radial and circular test motions were presented separately in interleaved constant stimulus sessions such that the type of motion component added (circular or radial respectively) was the same throughout a test session. Each constant stimulus session examined direction discrimination in one of four stimulus conditions, radial or circular test motions at two mean dot speeds; 8.4 and 30 °/s (= 0.68 ∗ max speed), and consisted of eight shifts (ϕ_p), in stimulus flow angle presented across 128 trials (16 trials per level). To minimize stimulus adaptation during a constant stimulus session, opposing test motions (e.g., expansion and contraction) were randomly interleaved across trials. Trials were presented in random order with the target motion equally likely to appear in either stimulus interval. In cases where the simplified criteria in Table 1 mixed clockwise and counter-clockwise judgments within a constant stimulus session (e.g., expanding and contracting test motions), observer's responses to test motions eliciting counter-clockwise judgments (e.g., contraction) were automatically inverted prior to analysis.

Each observer participated in at least eight constant stimulus sessions per stimulus condition with the order of conditions randomized across sessions. For each session, discrimination thresholds were computed as the change in flow angle (in degrees) necessary to discriminate shifts in motion direction with 82% probability.

3.1.2. Planar direction discrimination

In the GMP task the local motion of adjacent dots was approximately planar, changing by less than 10° within a one degree aperture near the stimulus center and less than 8° within a three degree aperture at the outer edge of the stimulus. Over such regions, the change in direction of the motion pattern stimuli was closely approximated by a change in planar motion direction. Under these conditions, GMP discrimination could be mediated by motion direction mechanisms selective to changes in the direction of simple planar motions and not necessarily to changes in the global motion pattern.

To control for the use of motion directions mechanisms in performing the GMP task, we also tested a subset of observers on a direction discrimination task. Here stimuli consisted of RDKs containing uniform planar motion presented in an 18° aperture. Dot speed was held constant across the stimulus aperture and set to the slower of the two mean dot speeds used in the GMP task (8.4 °/s). The test paradigm and all other stimulus properties were matched to the GMP task. The observers' task was to indicate which stimulus interval contained planar motion rotated counter-clockwise relative to the test motion.

Each constant stimulus session examined one of four directions of motion (up, down, left, right) and consisted of 96 trials uniformly distributed across six shifts in direction angle. Trials were presented in random order with the target motion equally likely to appear in either stimulus interval. Each observer participated in at least five constant stimulus sessions for each of the four motion directions.

On a frame-by-frame basis the changes in direction applied in the GMP and direction discrimination tasks were identical. During a stimulus frame, both implemented a fixed change in angular direction (ϕ_p) relative to a dot's original trajectory on that frame. In practice, however, the continuous change in local motion direction with polar angle necessary to form motion pattern stimuli meant that after each frame-wise displacement the dot's original direction of motion was slightly different. This resulted in a cumulative change in net

direction for complex motions that was slightly greater over the lifetime of a dot (Fig. 3).

From Eq. (2), the total displacement of a dot in the GMP task increased with distance from the stimulus center, such that at a mean dot speed of 8.4 °/s the range was 1–2°. Over the lifetime of a dot this resulted in a cumulative change in motion direction that was 7% greater than in the direction discrimination task. At the edge of the outer stimulus aperture the increase in the maximum *instantaneous* change of motion direction between frames was 13%. To correct for this effect GMP thresholds were scaled by 13% post hoc to ensure a con-servative comparison of any differences in performance between the two tasks.

3.2. Results

Discrimination thresholds for radial (expansion and contraction) and circular (clockwise (CW) and counter-clockwise (CCW)) motions were obtained at two mean dot speeds (8.4 and 30 °/s) in six observers. At both speeds, performance followed a distinct trend in the mo-tion pattern space with discrimination thresholds for ra-dial motions lower than for circular motions, (Fig. 4).
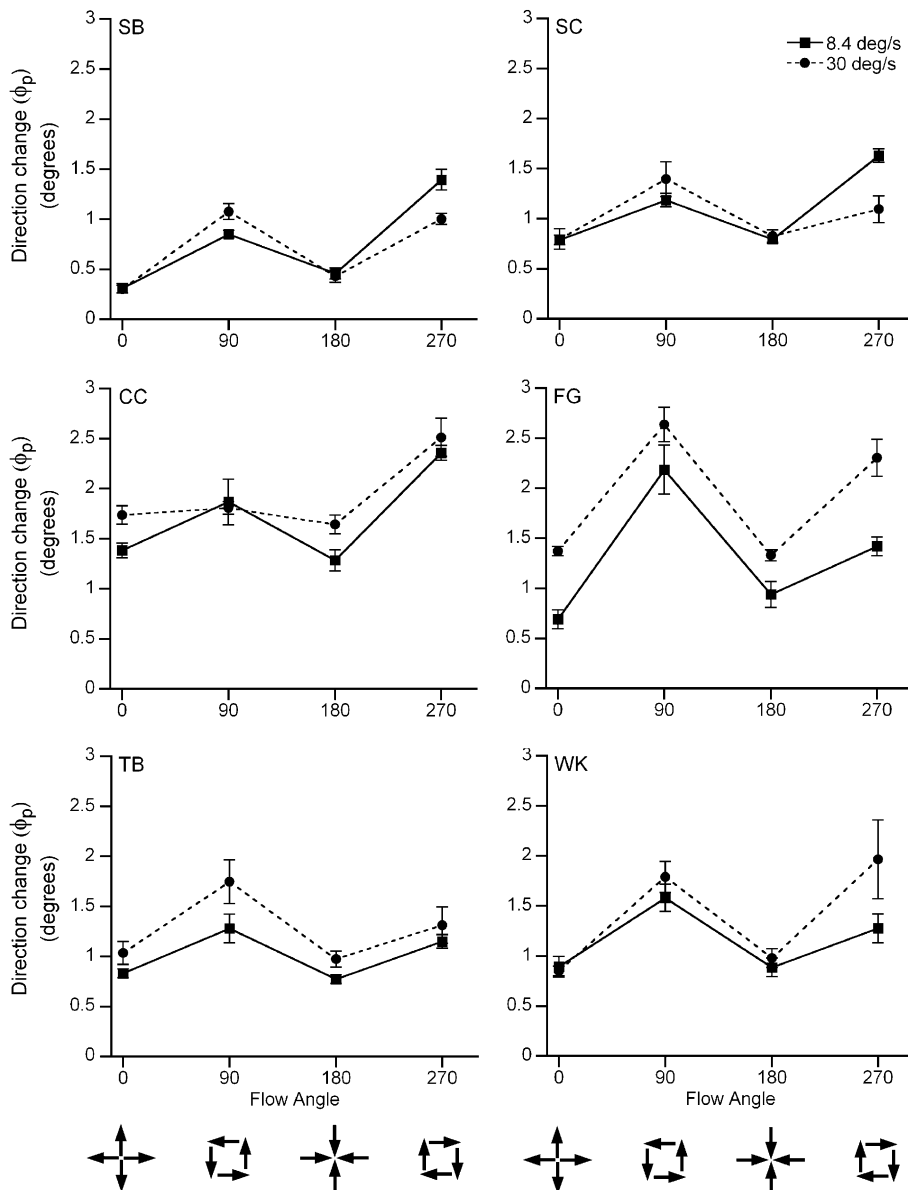
Fig. 4. GMP thresholds for radial and circular motions in six observers tested at two average dot speeds (squares—8.4 °/s; circles—30 °/s). The test motion is denoted by its flow angle (ϕ) in the motion pattern space; ϕ = 0°, 90°, 180°, and 270° for expansion, CCW rotation, contraction, and CCW rotation respectively. Performance is reported as the average threshold (ϕ_p) in degrees ±1 SE.

Across observers, thresholds for expansions/contractions and CW/CCW rotations were well matched ($\phi_{\rm p} \sim 0.5$–$1.5°$ and $\phi_{\rm p} \sim 1$–$2.5°$ respectively) and were robust to changes in the type of discrimination (CW versus CCW shifts by $\phi_{\rm p}$).

A two-way analysis of variance with the type of motion (radial versus circular) and speed (8.4 versus 30 °/s) as factors revealed that the difference between radial and circular thresholds was significant for all observers ($F(1, 73) \geqslant 21.23$, $p < 0.001$). Thresholds also tended to increase with speed, however, the difference was only significant for FG and TB (FG: $F(1,78) = 26.17$, $p < 0.01$; TB: $F(1,78) = 9.04$, $p < 0.01$; WK: $F(1,84) = 1.44$, $p > 0.05$; CC: $F(1,43) = 3.95$, $p > 0.05$; SC: $F(1,73) = 0.4$, $p > 0.1$; SB: $F(1,93) = 0.44$, $p > 0.1$). None of the observers showed a significant interaction between factors.

By comparison, direction discrimination thresholds for cardinal motions (i.e. up, down, left, and right) showed no effect of direction (Fig. 5). In both observers (one experienced, SB, and one naïve first-time observer, TB) direction discrimination thresholds were significantly higher than GMP thresholds ($t(33) = 2.42$, $p < 0.05$, one-sided). The difference was reduced when GMP thresholds were scaled to account for the cumulative change in local motion direction (Fig. 5; dashed line). With the exception of clockwise rotation for SB ($t(33) = 1.07$, $p = 0.15$), the resulting increase in GMP thresholds was not sufficient to account for the observed difference between planar and radial/circular motions.

3.3. Discussion

In the GMP task, the changes in direction applied to radial and circular test motions were functionally equivalent to the normalized vector addition of a small

orthogonal circular or radial motion respectively. This is computationally similar to the vector combination of orthogonal motion patterns used in masking studies by Freeman and Harris (1992) to examine motion pattern detection and later by Te Pas et al. (1996) in experiments examining observers' sensitivity to motion noise.

In their experiment, Freeman and Harris examined detection of a target motion as a function of the speed of an orthogonal motion pattern mask. In cases where the speed of the masking motion was significantly larger than the target motion, (their 8:1 speed difference) this was equivalent to detecting a small change in direction relative to the mask. Under these conditions, comparison of detection thresholds revealed differences between radial and circular motions that were qualitatively similar to those found in the GMP task. When radial and circular thresholds were converted to a common angular change in direction, motion detection for a slow circular 'target' added to a fast radial mask was consistently better than for a slow 'radial' target added to a fast circular mask (approximately 1.1 and 1.3° for subject TCAF respectively). This agrees well with our results and may suggest a difference in direction sensitivity between radial and circular motion mechanisms.

The difference might also suggest a psychophysical correlate to the bias for expanding motions in cortex. The equivalence between thresholds for expansions and contractions would seem to argue against such a relationship, however, this implicitly assumes a mechanism in which *independent* neural responses are pooled to extract information relevant to the task. Within cortex the high degree of inter-connections typically observed within visual areas makes this simplifying assumption of independence unlikely. Biologically constrained models tend to support this view, linking
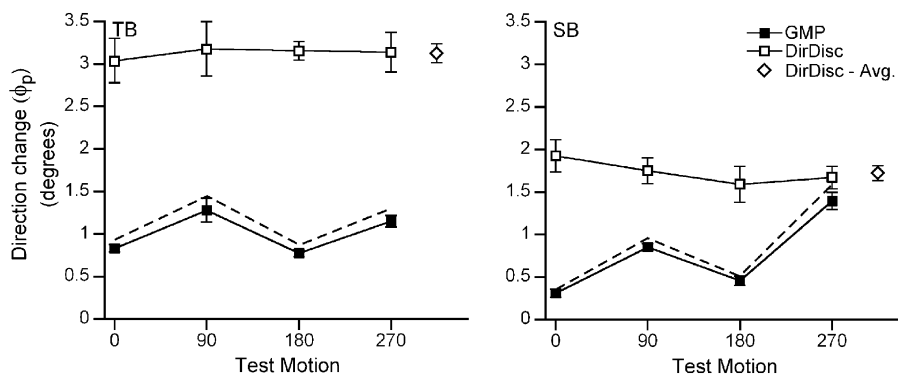
Fig. 5. GMP and direction discrimination thresholds for two observers. Stimuli were presented at 8.4 °/s in both tasks. The type of test motion is indicated along the abscissa; (ϕ) as in Fig. 4 for the GMP task (filled squares); test motion direction (0°, 90°, 180°, 270° for right, up, left, and down respectively) for the direction discrimination task (open squares). Thresholds in both tasks correspond to the frame-wise change in the angle of each dot's trajectory relative to the local direction of the test motion. Direction discrimination thresholds averaged across the four test directions are shown to the right for each observer (open diamond). GMP thresholds were scaled by 13% (dashed line), to equate the net change in dot trajectories between the two tasks (see Fig. 3).

inter-connected neural representations to psychophysical performance on motion pattern tasks (Beardsley & Vaina, 2001, 2004a, 2004b).

4. Experiment 2: Direction discrimination with spiral motions

Psychophysical studies of motion pattern coherence indicate that motion sensitivity is equivalent for cardinal motions (i.e., radial and circular) and significantly worse for intermediate spiral motions (Morrone et al., 1999). Summation and masking studies using overlapping orthogonal motions report similar differences (Burr et al., 2001), suggesting a cardinal representation for motion pattern processing, while others indicate that radial, circular, and spiral mechanisms are necessary to account for psychophysical performance in complex motion tasks (Meese & Anderson, 2002).

If motion pattern processing were mediated by cardinal mechanisms then we would expect GMP discrimination for spiral motions to follow one of two trends. Performance could be based on an independent threshold mechanism, in which the first detector to exceed a fixed response threshold signals the direction change. In this case, direction discrimination for off-axis spiral motions should be significantly worse than for radial or circular motions, similar to motion pattern coherence tasks (Burr et al., 2001; Morrone et al., 1999). Alternatively, if performance were based on a simple pooling across cardinal motion mechanisms then discrimination for spiral motions should be significantly better than for radial or circular motions.

The latter prediction follows from the fact that for detectors with moderate bandwidths, the region of greatest sensitivity occurs away from the preferred motion where the slope of the detector's response is greatest. For radial and circular motion detectors with bandwidths of 46° (Meese & Anderson, 2002; Meese & Harris, 2001a), the region of greatest direction sensitivity coincides with spiral motions. Fig. 6A illustrates the predicted GMP thresholds for simple pooling model consisting of four detectors separately tuned to expanding, contracting, and rotating motion (see Appendix A for details).

If GMP discrimination is not mediated by cardinal mechanisms but instead by a more distributed representation then we would predict that thresholds for spiral motion be similar across test motions (Fig. 6B), (see also, Beardsley & Vaina, 2004a, 2004b). In this case systematic changes in thresholds as a function of test motion would suggest variations in the sensitivity and/or distribution of the motion pattern mechanisms involved in the task.

4.1. Methods

To determine whether a cardinal representation of motion pattern mechanisms is sufficient to account for GMP performance we performed a more detailed sampling of the stimulus space using a set of eight test motions (radial, circular, and four intermediate spiral motions). The basic stimulus and experimental paradigm were the same as in Experiment 1. As in the first experiment observers' discrimination criterion were simplified conceptually based on the addition of orthogonal radial (expansion/contraction) or circular (clock-
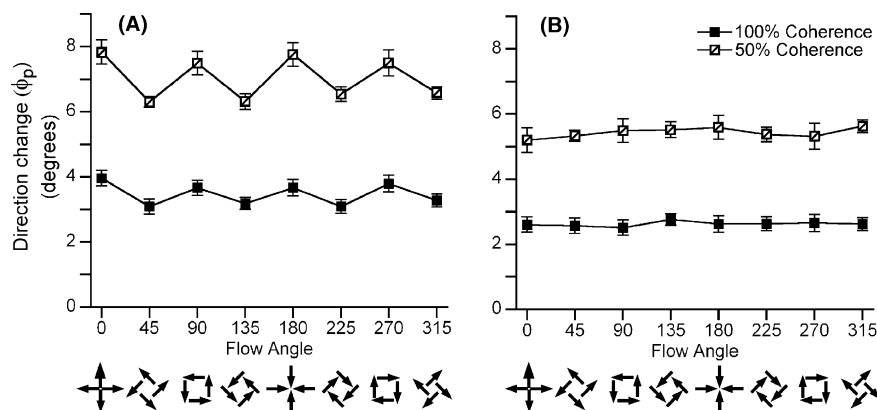
Fig. 6. Cardinal (radial and circular) and spiral GMP thresholds predicted for a simple pooling model based on four (cardinal model) or eight (cardinal + spiral model) evenly spaced motion pattern mechanisms. (A) A cardinal representation predicts that thresholds for coherent spiral motions be significantly lower than those for radial and circular motions (filled squares). For detector responses that are a proportional to motion coherence, the addition of stimulus noise (50% coherent condition—hatched squares) scales thresholds inversely with coherence such that the difference between cardinal and spiral thresholds is increased on a linear scale. (B) A cardinal + spiral representation predicts similar performance across test motions.

wise/counter-clockwise rotations) motion components. In the case of spiral test motions, observers were required to indicate the stimulus interval containing either a larger radial or circular motion component (Table 1).

In a second series of tests we examined GMP thresholds for radial, circular and spiral motions using stimuli containing 50% coherent motion embedded in a flicker noise (Newsome & Pare, 1986; Morrone et al., 1995; Burr et al., 1998; Morrone et al., 1999). If motion pattern processing is mediated by cardinal motion mechanisms, a pooling model would predict that discrimination thresholds should increase more for cardinal than for spiral motions in the presence of motion noise. For a linear change in detector response with motion coherence, similar to that reported in area MT (Britten, Shadlen, Newsome, & Movshon, 1993), the model predicts that thresholds should scale inversely with motion coherence (Fig. 6).

In the motion noise condition stimuli were created by randomly assigning dots as 'signal' or 'noise' on a frame-by-frame basis such that the proportion of signal dots in

each frame was 50%. For each stimulus frame, signal dots were assigned velocities consistent with the motion pattern being presented and noise dots were randomly repositioned within the stimulus aperture. Across the population of dots, this resulted in a decreasing probability of uninterrupted local motion for the ith dot (d_i)

$$P(d_i) = \left[\frac{C_p}{100\%} \right]^n \qquad (3)$$

that was a function of the motion pattern coherence (C_p) and the number of consecutive signal frames (n). For the 50% motion coherence used here the probability of an uninterrupted local dot motion across three or more frames was low (12.5%), limiting observers' ability to make local direction discriminations based on individual dot trajectories.

4.2. Results

Discrimination thresholds for the extended set of test motions were obtained at both dot speeds (8.4 and
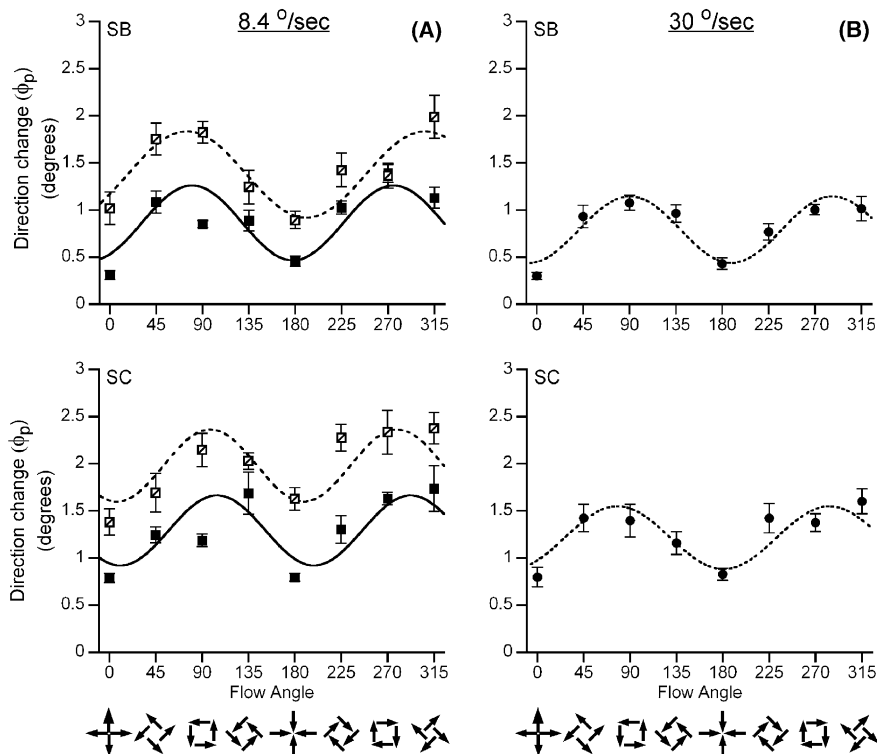
Fig. 7. GMP thresholds across eight test motions and two mean dot speeds (8.4 and 30 °/s—filled circles and squares respectively) for two observers (SB and SC). Test motions are represented by their corresponding flow angles as in Fig. 4. Flow angles of 45°, 135°, 225°, and 315° correspond to spiral test motions. (A) Direction discrimination as a function of test motion for stimuli with a mean dot speed of 8.4 °/s. Thresholds are plotted for two stimulus conditions; 100% (filled squares) and 50% (hatched squares) coherent dot motion. Thresholds in both conditions were well fit (solid and dashed lines respectively) by a sinusoid function of the form $y = A \sin(k\phi + \theta) + C$ where ϕ is the test flow angle, and A, k, θ, and C are the amplitude, frequency, phase, and offset respectively. (B) Direction discrimination as a function of test motion for stimuli with a mean dot speed of 30 °/s. Thresholds were well fit by sinusoids (dotted line) whose amplitude, phase, and offset were similar to those in (A).
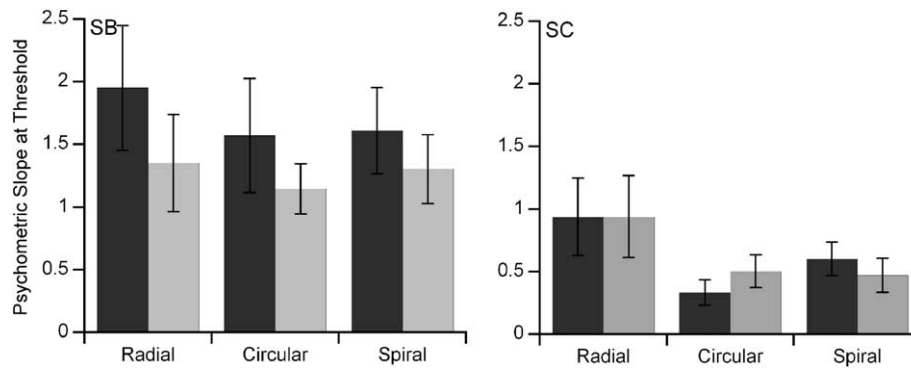
Fig. 8. Psychometric slopes (at threshold) as a function of stimulus class in two observers (SB and SC). Slopes are reported as the change in proportion correct per degree change in flow angle and correspond to the mean ($n \geqslant 18$) ± 1 SE across all test motions within each stimulus class (e.g., radial—expansion and contraction). Light and dark bars indicate slopes for stimuli presented at 8.4 and 30 °/s respectively.

30 °/s) in two experienced psychophysical observers (Fig. 7). In both observers, performance followed a consistent trend across the motion pattern space with discrimination thresholds for radial motions ($\phi = 0°$, 180°) lowest and those for circular motions ($\phi = 90°$, 270°) among the highest. Individual thresholds for the intermediate spiral motions were not significantly different from their circular motion counterparts ($t(60) = 0.75$, $p > 0.1$). However, the trends across test motions were well fit ($r^2 > 0.59$) by sinusoids whose average amplitude, period and phase were $0.36 \pm 0.06°$, $198 \pm 20°$ and $-75 \pm 41°$ respectively.

Equivalent trends in performance were obtained when stimuli were presented with 50% coherence (Fig. 7A). Thresholds were well fit ($r^2 > 0.61$) by sinusoids whose periods and phases were (SB: $231 \pm 21°$ and $-27 \pm 27°$; SC: $181 \pm 19°$ and $-104 \pm 48°$) respectively. In both observers, thresholds increased by a fixed interval across test motions ($p < 0.001$; Tukey–Kramer), and did not significantly alter the amplitude of the resulting sinusoidal trend. This result contrasts with the linear scaling of discrimination thresholds with motion coherence predicted by a cardinal pooling model (Fig. 6A), and together with the consistency of the sinusoidal trend across test conditions suggests a more distributed representation of motion pattern mechanisms.

Examination of observers' sensitivity to ϕ_p via the psychometric slope, is consistent with this interpretation. In both observers slopes for spiral motions were bounded by those radial and circular motions (Fig. 8). Analysis post hoc revealed no significant difference between radial, circular, and spiral motions for SB ($F(2,181) = 1.53$, $p = 0.22$), although slopes did increase with dot speed ($p < 0.005$; Tukey–Kramer). For SC, radial motion slopes were significantly higher than those for spiral and circular motions ($p < 0.05$; Tukey–Kramer), but there was no effect of dot speed ($F(1,145) = 1.3$, $p = 0.26$).

4.3. Discussion

The similarity between cardinal and spiral thresholds, together with the constant increase in thresholds with motion noise is generally inconsistent with predictions based on a cardinal representation of motion pattern mechanisms. This agrees well with summation and adaptation studies suggesting that radial, circular, *and* spiral mechanisms are necessary to account for psychophysical performance in complex motion tasks (Meese & Anderson, 2002; Snowden & Milne, 1996). However, even with the inclusion of spiral motion mechanisms (Fig. 6B), the consistent change in thresholds with test motion is not readily accounted for.

It may be that there is an intrinsic difference in direction sensitivity between radial, circular, and spiral motion mechanisms. This would be the most parsimonious explanation, however, it would seem inconsistent with the similarity in psychometric slopes between the three types of motion. The alternative is that the change in threshold with test motion reflects an underlying difference in the distribution of motion pattern detectors across the stimulus space. Such differences would seem reasonable in light of the consistent bias for expanding motions reported in cortex (Anderson & Siegel, 1999; Duffy & Wurtz, 1991a; Geesaman & Andersen, 1996; Graziano et al., 1994; Read & Siegel, 1997; Schaafsma & Duysens, 1996; Siegel & Read, 1997), however, as we discussed in Experiment 1 the relationship between the radial motion bias reported here and the preference for expanding motions in cortex is not necessarily direct.

5. Experiment 3: Influence of the radial speed gradient

An implicit global property of the dot motion equations in Eq. (2) is the presence of a radial speed gradient in which dot speed increases with distance from the stim-

ulus center. Computationally, the presence of the speed gradient is uninformative regarding the changes in direction measured in the GMP task. As such we would expect little if any impact on performance when the speed gradient is removed.

5.1. Methods

To quantify the effect of the speed gradient we tested a subset of observers from Experiment 1 using a modified set of radial and circular test motions. The stimulus and experimental paradigm were the same as in Experiment 1 with the exception that here the speed gradient was removed. In this condition, referred to as random speed, dots were assigned a fixed speed based on their location in the speed gradient and then their initial (x, y) positions were randomly shuffled within the stimulus aperture. This resulted in stimuli whose global distribution of directions *and* speeds was the same as Experiment 1, but whose spatial distribution of speeds was random.
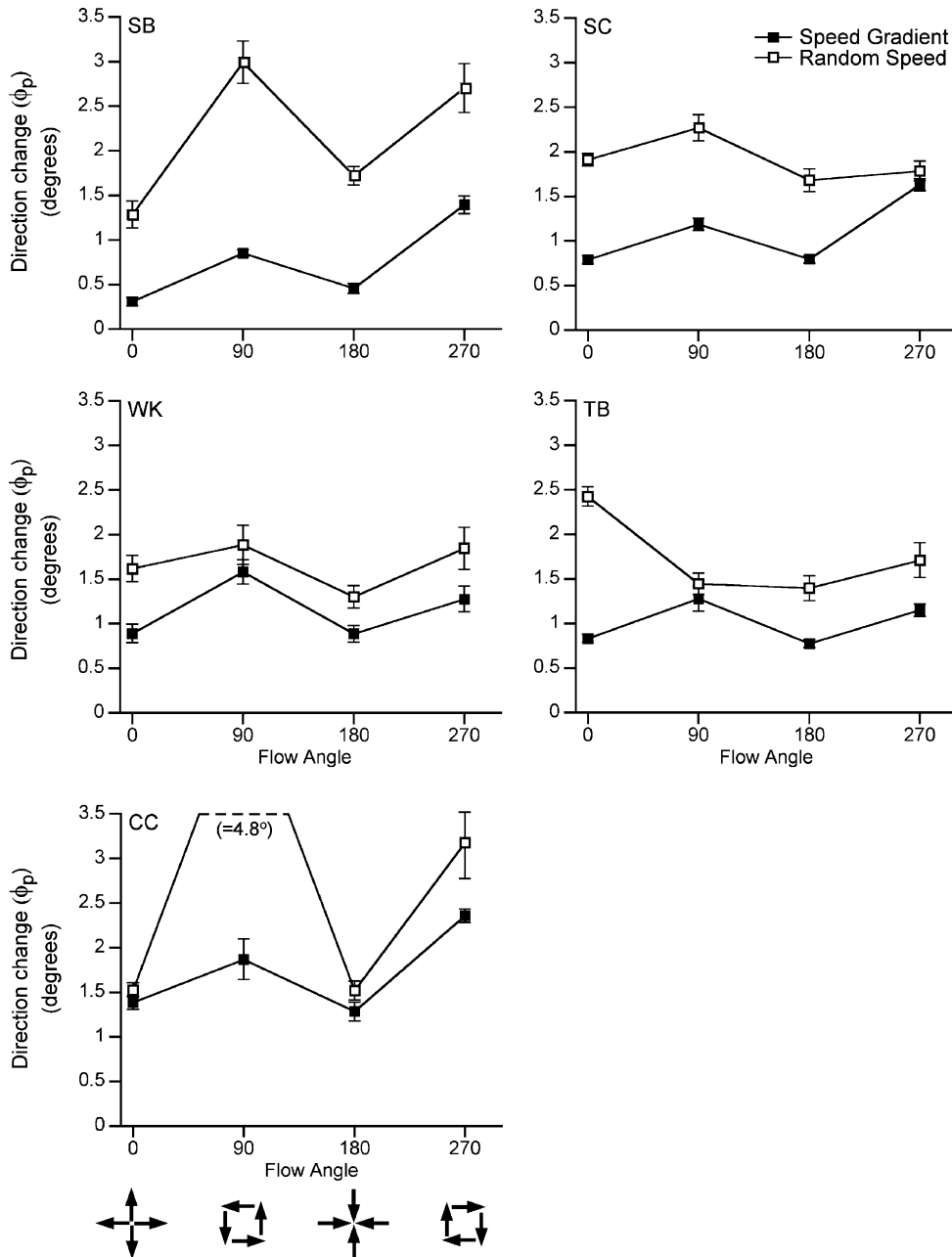
Fig. 9. GMP thresholds for stimuli with (filled squares) and without (random speed condition—open squares) a radial speed gradient (mean dot speed = 8.4 °/s) in five observers. In the random speed condition, dots were assigned fixed speeds based on their location in the speed gradient and then their initial (x, y) positions were randomly shuffled. The resulting stimulus contained the same global distribution of directions and speeds without the radial increase in speed with distance from the stimulus center. Thresholds increased for all observers when the speed gradient was removed. In three observers (SB, CC, and TB), the increase was greater for circular motions than for radial motions.

5.2. Results

Fig. 9 shows radial and circular GMP thresholds with and without the radial speed gradient for five observers. When the speed gradient was removed (random speed condition) thresholds consistently increased. Subject specific ANOVAs revealed a significant main effect of the speed gradient (Table 2), with thresholds for both radial and circular motions significantly higher in the random speed condition in all observers (all $p < 0.05$; Tukey–Kramer). Three observers (SB, CC, and TB) also exhibited a significant interaction between test motion and speed gradient, in which the increase in random speed thresholds was greater for circular motions than for radial motions (Table 2).

The proportion change in thresholds calculated as a weighted population average across observers is shown in Fig. 10A. When the speed gradient was removed GMP thresholds increased by approximately 50%. Fig. 10B shows the class averaged slopes (at threshold) for the random speed condition plotted as a function of the speed gradient condition for each observer. In all cases slopes were located along or below the diagonal with unit slope indicating a general decrease in observer sensitivity to ϕ_p when the speed gradient was removed.

5.3. Discussion

The consistent effect of the speed gradient on observers' performance is interesting given the spatial symmetry implicit in the stimulus design. Since the speed gradient was a function of distance from the stimulus center-of-motion, its distribution was radially symmetric for all motion patterns. Under these conditions the speed gradient did not contribute computationally relevant information to the GMP task. However, it did convey information regarding the integrative structure of the global motion field. As such, the increase in thresholds for the random speed condition may suggest a common preference in the underlying motion mechanisms for spatially structured speed information.

This interpretation is consistent with the preference of motion pattern cells for stimuli containing radial

Table 2
Two-way ANOVA of GMP thresholds when the speed gradient was removed from the stimulus

Subject	d.f.	Main effect of speed gradient		Main effect of motion (radial versus circular)		Interaction (gradient × motion)	
		F	p	F	p	F	p
SB	(1,91)	182.7	≪**0.001**	99.1	≪**0.001**	9.3	**0.003**
CC	(1,42)	7.2	**0.01**	18.6	**<0.001**	5.0	**0.031**
TB	(1,77)	56.8	≪**0.001**	0.1	0.79	15.1	**<0.001**
WK	(1,78)	20.8	≪**0.001**	18.1	**<0.001**	0.4	0.55
SC	(1,58)	74.2	≪**0.001**	10.3	**0.002**	0.7	0.42

Factors were type of motion (radial versus circular) and distribution of speeds (speed gradient versus random speed). Significant effects are shown in bold.
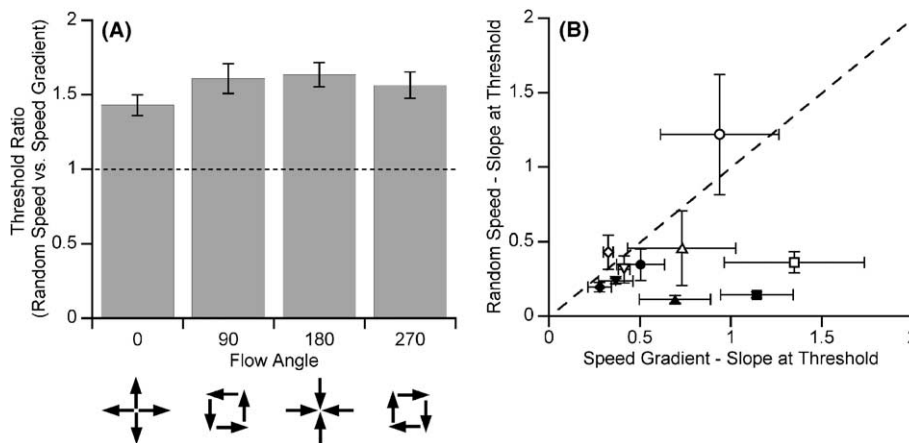
Fig. 10. (A) Proportion change in radial and circular thresholds when the speed gradient was removed. Performance is plotted as the weighted population average across five observers. In all cases removing the speed gradient increased GMP thresholds by approximately 50%. (B) Class averaged slopes (at threshold) for the random speed condition plotted as a function of the slopes with the speed gradient for five observers. Units of slope are the same as in Fig. 8. Each symbol type (circle, square, etc.) indicates the mean slope ±1 SE for a single observer. Open symbols correspond to radial test motions and filled symbols correspond to circular test motions. In all cases slopes were located along or below a diagonal line with unit slope (dashed line) indicating a general decrease in observer sensitivity with the removal of the speed gradient.

speed gradients. In single cell studies, Duffy and Wurtz (1997) found that a majority (89%) of neurons in MSTd preferred stimuli with either negative or positive speed gradients. The effect of the speed gradient was typically modulatory with over half of neurons exhibiting gradient versus non-gradient response ratios less than two (Fig. 5c; Duffy & Wurtz, 1997). The threshold ratio of 1.5 observed here agrees well this figure.

The increase in thresholds for the random speed condition could also be due to mechanisms that 'dislike' the randomized distribution of speeds. While the structure of the random speed stimulus does not preclude this possibility, the results of similar experiments examining the effects of velocity gradients on optic flow processing suggests this is generally not the case. Using radial and circular motions, Rodriguez-Sanchez, Tsotsos, and Martinez-Trujillo (2004) examined the ability of observers to discriminate changes in direction for stimuli with and without a radial speed gradient. In the gradient condition dot speed increased with distance from the stimulus center while in the 'no-gradient' condition all dots moved at a single constant speed. They found that discrimination thresholds for radial and circular motions were on average 20% higher for constant speed stimuli than for stimuli containing a speed gradient. This increase is generally consistent with the results reported here and further suggests a common preference among motion pattern mechanisms for structured speed information.

6. General discussion

In the experiments presented here we have shown that the ability of observers to discriminate changes in motion pattern direction changed as a function of the test motion pattern. In all observers discrimination thresholds for radial motions were consistently lower than for circular motions independent of dot speed, the presence of a radial speed gradient, or motion noise. The consistency and extent of this difference is intriguing for two reasons. First it is reminiscent of the bias for expanding motions reported in motion pattern responsive areas of cortex (Anderson & Siegel, 1999; Geesaman & Andersen, 1996; Graziano et al., 1994; Read & Siegel, 1997; Schaafsma & Duysens, 1996; Siegel & Read, 1997). Second, the variation between radial and circular motions appears significantly different from motion pattern coherence experiments, which presumably utilize similar mechanisms.

In motion pattern coherence tasks, thresholds for detection and/or discrimination of radial and circular motions are typically well matched while those for spiral motions tend to be significantly higher, consistent with the use of radial and circular motion pattern mechanisms (Burr et al., 2001; Morrone et al., 1999). Sub-threshold summation studies generally agree with these results but also suggest the presence of spiral motion mechanisms that are either fewer in number or less sensitive than their radial and circular counterparts (Burr et al., 2001; Meese & Anderson, 2002).

By comparison, in the GMP task direction discrimination thresholds for spiral motions consistently fell between those for radial and circular motions, resulting in a sinusoidal trend across the motion pattern space whose periodicity indicates a radial bias in psychophysical performance. The corresponding psychometric slopes agreed closely with the similarity between spiral and radial/circular thresholds and suggest that direction sensitivities for radial, circular, and spiral motion mechanisms are comparable. This is generally consistent with motion pattern selective neurons in areas such as MSTd, for which both the width of motion pattern tuning and relative numbers (by class) of radial, circular, and spiral neurons are similar (Geesaman & Andersen, 1996; Graziano et al., 1994).

At a psychophysical level, the motion specific differences in GMP versus motion pattern coherence tasks can be in part accounted for by the different types of visual motion properties measured; direction versus noise sensitivity. Thus while both tasks may probe the same motion pattern mechanisms, they may do so along different stimulus dimensions such that the GMP task measures direction sensitivity across neighboring motion mechanisms that respond to similar motions while the motion pattern coherence task measures external noise sensitivity between disjoint and/or opposing motion mechanisms, e.g., expansion versus contraction.

This difference may also explain the seeming incongruity between performance in motion pattern coherence tasks and the visual motion properties of neurons in motion pattern responsive areas of the cortex. Specifically, the detection of coarse direction differences in the motion coherence paradigm might not lend itself to direct comparison with motion pattern biases reported using fully coherent stimuli.

We propose that near the coherence threshold, the interaction between neural response profiles for motion pattern tuning and coherence attenuates all but the most responsive cells, resulting in a winner-take-all response similar to that proposed by Burr et al. (2001). This may account for both the lack of a perceptual correlate to the expansion bias in motion pattern coherence tasks and the equivalence between radial and circular thresholds if, as the neurophysiology suggests, motion pattern sensitivity across neurons is similar. It would also account for the differences between motion coherence and GMP results since in the latter case performance was obtained at supra-threshold coherence levels for which motion pattern tuning properties would dominate. As coherence decreases near threshold we would predict that the radial motion bias observed in

the GMP task should be systematically reduced. Similarly the effect of the speed gradient should also decrease as coherence, and not structured speed, progressively dominates attenuation of the motion pattern response.

6.1. The pattern of GMP thresholds favors a global motion pattern mechanism

At first glance the ability of human observers to accurately discriminate small changes in the direction of individual and groups of translating dots would appear to limit the interpretation of GMP results within the context of a motion pattern specific mechanism. In direction discrimination tasks thresholds for cardinal motion directions (up, down, left, and right) are similar, typically spanning a range of 1–2° (Ball & Sekuler, 1979; De Bruyn & Orban, 1988; Watamaniuk et al., 1989). While such performance in generally consistent with the range of GMP thresholds reported here (0.5–2°), direct comparison within observers indicates that GMP thresholds are consistently lower than those for translating motion (Fig. 5).

Direction specific biases have also been reported whose relative differences are reminiscent of the threshold variations observed here. Several groups have demonstrated the existence of an oblique effect in which direction discrimination thresholds for off-axis directions are significantly higher than those for on-axis (cardinal) directions (Ball & Sekuler, 1987; Coletta, Segu, & Tiana, 1993; Gros, Blake, & Hiris, 1998; Matthews & Qian, 1999; Matthews & Welch, 1997).

Still others have reported a centripetal bias in sensitivity to motion coherence that is most pronounced for eccentricities less than 12° (Barton, Sharpe, & Raymond, 1996; Edwards & Badcock, 1993; Raymond, 1994; Vaina, Cowey, Eskew, LeMay, & Kemper, 2001; Zhao et al., 1995). However, it is less clear whether such biases exist in the case of direction discrimination. Using central and peripheral stimuli (10° eccentricity), Gros et al. (1998) showed that thresholds for oblique directions were always higher than for cardinal directions, irrespective of location in the visual field. Their results argue against a centrifugal bias in direction discrimination but do not directly address the existence of a centripetal bias in the task.

Together these results suggest a host of direction specific differences that could potentially account for the motion specific change in GMP thresholds. The apparent similarities between GMP thresholds and motion direction specific effects together with the coherent stimulus structure of Experiment 1, would seem to suggest a primary role for motion direction, as opposed to motion pattern, mechanisms in the task. However, closer examination of the stimulus structure and pattern of GMP thresholds indicates that this is not the case.

In the GMP task, the 2-D continuum of local motion directions was uniformly represented within the central 24° stimulus. Globally, each motion pattern was comprised of the same set of symmetrically positioned local motion directions and was uniquely defined only by the spatial locations of directions within the visual field. Within this structure, cardinal and oblique directions are simultaneously present in all stimuli making systematic threshold differences associated with an oblique effect unlikely.

If, on the other hand, observer performance were mediated by attending to a spatially localized subset of motion directions, the oblique effect would predict significant variations in threshold performance across motion patterns. Under these conditions the local motion symmetry implicit in the motion pattern stimuli would predict a grouped difference between cardinal and spiral motions that would be dependent on the region of the stimulus used to perform the task. This is because the motion directions present within any region of the display do not shift between on and off-axis (i.e. cardinal and oblique) directions for stimuli separated by 90° in the motion pattern space. In radial and circular motion patterns, for example, the local directions present in a region located to the right of the fixation always contained on-axis cardinal motion directions (Fig. 11).

Finally, the presence of a centripetal bias in direction discrimination would predict that thresholds for contracting motions be lower than those for expanding motions. This did not occur. Alternatively, direction discrimination within the central 24° may be homogeneous, consistent with the representation in direction selective cortical areas such as MT (Albright, 1989). Under these conditions the uniform presentation of all motion directions would predict discrimination thresholds that are independent of the motion pattern presented in the task (Beardsley and Vaina, unpublished simulations).

The inability of motion direction specific mechanisms to account for the observed differences between radial and circular thresholds supports a primary role for motion pattern specific mechanisms in the GMP task. This is consistent with psychophysical studies of motion pattern coherence which indicate the existence of motion pattern specific mechanisms distinct from those that process motion direction (Burr et al., 2001; Burr et al., 1998; Meese & Anderson, 2002; Meese & Harris, 2001a, 2001b; Morrone et al., 1999; Morrone et al., 1995).

6.2. Psychophysical correlates to complex motion processing in cortex

Observers' performance on the GMP tasks suggests several similarities between the motion pattern mechanisms inferred here and the preference of neurons to
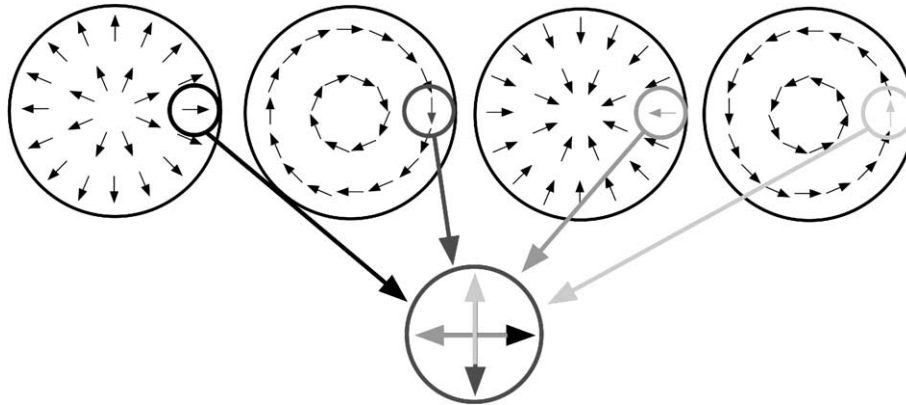
Fig. 11. An example of relative local motion constancy (axial versus oblique) across motion pattern stimuli. For a localized region to the right of the stimulus center, the local motion directions are axial (left, right, up, down) across radial and circular test motions. More generally, within any spatially localized region, the motion direction components across orthogonal test motions (i.e., separated by 90° of flow angle) are themselves orthogonal.

complex motion reported in the cortex of non-human primates. The trends in GMP performance as a function of test motion, speed and the presence of a radial speed gradient can all be correlated to visual motion properties reported in MSTd and other motion pattern responsive areas, such as ventral intraparietal cortex (VIP), anterior superior temporal (STPa) cortex, and area 7a.

Within these regions, neurons typically have large receptive fields and exhibit strong preferences for radial, circular, spiral, or planar motions (Anderson & Siegel, 1999; Duffy & Wurtz, 1991a; Graziano et al., 1994; Schaafsma & Duysens, 1996; Siegel & Read, 1997); for a review see (Raffi & Siegel, 2004). Qualitatively, the distributions of preferred motions in VIP, STPa, and area 7a are similar to the bias for expanding motions reported in MSTd (Graziano et al., 1994; Geesaman & Andersen, 1996; Tanaka, Fukada, & Saito, 1989; Tanaka & Saito, 1989). Furthermore, neurons in these areas are responsive across a wide range of speeds and exhibit scale invariance to changes in the size of the visual stimulus (Duffy & Wurtz, 1991b; Graziano et al., 1994; Schaafsma & Duysens, 1996). Given these similarities and the relative abundance of motion pattern studies in MST versus VIP, STPa, and area 7a, we will concentrate the subsequent discussion on psychophysical correlates to the former.

The pattern of GMP thresholds shown in Figs. 4 and 7 (Experiments 1 and 2) indicate a preference for radial motions that is qualitatively similar to the bias for expanding motions reported in MSTd. Although the trend does not precisely match the distribution of preferred motions in MSTd, the similarity is compelling. The primary difference between the two profiles lies in the relative differences between radial GMP thresholds and the number of neurons preferring expansions versus contractions. Even the more conservative expansion bias reported by Geesaman and Andersen (1996) suggests a

difference between discrimination thresholds for expanding and contracting motions that is not observed here in our data. However, this implicitly assumes a context in which *independent* neural responses are pooled to extract information relevant to the task. Within the cortex the high degree of inter-connections typically observed within visual areas makes this simplifying assumption of independence unlikely.

Using a biologically constrained model of motion pattern processing we have shown that an expansion biased population of MSTd-like neurons can in fact account for psychophysical performance (Beardsley & Vaina, 2001, 2004a, 2004b). We compared GMP thresholds with equivalent measures of psychophysical performance in simulated neural populations that varied the strength of the expansion bias, population size, and the presence and structure of recurrent connections. As expected observer performance could not be accounted for by independently responding neurons and/ or by populations that did not contain an expansion bias. However, robust performance that was well matched to observes did occur for populations that combined an expansion bias with a simple inter-connected neural structure in which the strength of inhibition was a function of the relative difference in preferred motions between neurons.

In addition to the radial motion bias, Experiment 3 showed a consistent increase in GMP thresholds and decrease in psychometric slope when the radial speed gradient was removed (Figs. 9 and 10). Given the fact that the speed gradient itself did not contribute information relevant to the task, the observed decrease in sensitivity suggests an inherent preference in the underlying computational mechanisms for complex motions that contain structured speed information.

Similar preferences for spatially structured speed information have been reported in MSTd with a majority

of neurons (89%) preferring either negative or positive speed gradients (Duffy & Wurtz, 1997). The effect of the speed gradient was typically modulatory with responses for over half of neurons increasing by a factor of two or less (their Fig. 5c). The threshold ratio of 1.5 observed here agrees well this figure and further suggests a link between GMP discrimination and an MSTd-like neural representation in the human visual system.

6.3. GMP discrimination during visually guided navigation

In real-world environments the visual scene is often cluttered with object motions that are unrelated to an observer's self-motion. Under these conditions, the optic flow field contains not only the observer's self- and extra-retinal motions but also locally coherent object motions. Within such environments the ability to discriminate small changes in the global motion pattern could be used to aid motion-based segregation of the visual scene. Bravo (1998), found that observers were able to more easily locate inconsistent directions in spiral motions than in deformations, suggesting that mechanisms sensitive to the spiral motion pattern and not local direction differences were used to detect the discrepant motion. The ability to detect such motion differences and parse them from the global flow field could be used during visually guided navigation to reduce visual motion noise associate with irrelevant object motions.

Template matching models of self-motion estimation, such as that proposed by Perrone and Stone (1994, 1998), suggest that the ability to discriminate small changes in the global optic flow could play a more direct role in motion-based estimates of heading. In their model, Perrone and Stone showed that heading could be accurately estimated using a population of MSTd-like complex motion detectors acting as templates for specific instances of self-motion through the visual scene. Within this scheme, small changes in an observer's heading would introduce systematic shifts in the motion pattern direction of the resulting optic flow that would be reflected by a corresponding change in the template responses. In this context, sensitivity to the types of simple motion patterns used here arise as a computational by-product from cortical mechanisms optimized to dissociate self-motion from the visual scene and estimate heading. This interpretation is consistent with models proposed by ourselves and others linking complex motion perception to neural structures in MT/MSTd (Beardsley & Vaina, 2001, 2004a, 2004b; Lappe & Duffy, 1999; Perrone & Stone, 1998; Zemel & Sejnowski, 1998) and may suggest a common neural representation linking psychophysical mechanisms for simple motion pattern attributes with their more ecologically relevant counterparts.

Appendix A

Here we describe a simple pooling model of motion pattern discrimination. The model is intended to provide a first order comparison of the expected trends in GMP thresholds for two proposed distributions of motion pattern mechanisms. The first consists of a cardinal representation of four motion pattern detectors tuned to expansion, counter-clockwise rotation, contraction, and clockwise rotation ($\phi = 0°$, $90°$, $180°$, and $270°$ respectively). The second contains a more distributed representation of eight motion pattern detectors that includes detectors tuned for intermediate spiral motions.

Direction sensitivity was assumed to be the same for all motion pattern mechanisms. Both models also assume that direction discrimination is limited by internal noise whose mean and variance is constant for all motion pattern mechanisms. Direction bandwidths are drawn from best-fit cardinal and cardinal + spiral models developed by Meese and Anderson (2002) to examine motion pattern coherence.

A.1. Cardinal model of GMP discrimination

To simulate a cardinal representation of motion pattern mechanisms, four detectors tuned to expansion, counter-clockwise rotation, contraction, and clockwise rotation were spaced in 90 intervals across the motion pattern space ($\phi = 0°$, $90°$, $180°$, and $270°$ respectively). Each detector consisted of a Gaussian direction tuning function whose amplitude was proportional to stimulus coherence

$$R_i(\phi, c) = R_{ax}(c)e^{-(\phi-\phi_i)^2/2\sigma^2} + N_i \qquad (4)$$

where R_i is the response of the ith detector to a motion pattern stimulus with flow angle (ϕ), R_{max} is the detector's maximum response as a function of the proportion of coherently moving dots (c), ϕ_i is the flow angle of the detector's preferred motion, σ is the standard deviation of the detector response in the motion pattern space, and N_i is an independent source of internal noise.

Consistent with single cell studies in cortex (Britten et al., 1993), detector responses were assumed to be proportional to coherence. For simplicity, $R_{max} = c$, such that for fully coherent motion the gain was one. Standard deviation was set to $54°$ for all detectors, corresponding to the best-fit half amplitude bandwidth of $64°$, reported by Meese and Anderson (2002). The inter-

nal noise was assumed to be a Poisson process across stimulus trials with mean and variance scaled to $0.2 * R_{max}$ for fully coherent motion (Beardsley & Vaina, 2004a).

The GMP task was simulated using a vector summation rule to decode estimates of the stimulus flow angle from the model. After a stimulus presentation the response of each detector was used to weight its preferred motion expressed as a unit vector in the motion pattern space $\hat{\phi}_i$. The estimate of stimulus flow angle was then given by the vector sum of weighted responses across detectors.

$$\hat{\phi} = \sum_{i=1}^{4} R_i \hat{\phi}_i \qquad (5)$$

The experimental paradigm was the same as in Experiments 1 and 2. Psychophysical responses were obtained from the model for each test motion according to the clockwise change in flow angle criterion specified in the GMP task. For each constant stimulus session, discrimination thresholds were computed using a least-squares fit to percent correct performance across stimulus levels.

GMP performance was examined for the eight test motions described in Experiment 2 at two coherence levels (100% and 50%). Five simulations were run with 10 constant stimulus sessions for each experimental condition. Performance was reported as the mean threshold ± SE averaged across simulations. From Fig. 6A the cardinal pooling model predicts that direction discrimination be better for spiral than for cardinal motions. This follows directly from the increased slope of the direction tuning function for motions adjacent to the detector's preferred cardinal motion. From Eq. (4), the difference in slope between cardinal and spiral motion thresholds is a nonlinear function of the direction tuning bandwidth with a maximum sensitivity for spiral motions when $\sigma = 45°$. For larger values of σ, direction sensitivity for cardinal and spiral motions become more similar, however, the model predicts that sensitivity for spiral motions should always better than for cardinal motions.

When motion noise is added (50% coherence condition) the model predicts that GMP thresholds increase. To a first approximation the increase is inversely proportional to the change in coherence. In terms of absolute thresholds, the result is an increased difference between cardinal and spiral thresholds, with thresholds for cardinal motions increasing more than for spiral motions.

A.2. Spiral model of GMP discrimination

In an extension of the four-channel model, performance was also examined for the case of eight motion pattern mechanisms (4 cardinal + 4 spiral). In addition to the four cardinal detectors for radial and circular motion ($\phi = 0°$, 90°, 180°, and 270°), the model also contained four spiral detectors evenly spaced at 45° intervals between cardinal detectors ($\phi = 45°$, 135°, 225°, and 315°). The standard deviation of the direction tuning functions was set to 39°, corresponding to the best-fit half amplitude bandwidth of 46° reported by Meese and Anderson (2002) for eight motion mechanisms. All other detector properties and simulation procedures were that same as in the cardinal model.

For motion pattern mechanisms with equal sensitivity, the spiral model predicts that cardinal and spiral GMP thresholds be similar (Fig. 6B). As in the cardinal model discrimination thresholds scaled in inverse proportion to the motion coherence.

References

Albright, T. D. (1989). Centrifugal directional bias in the middle temporal visual area (MT) of the macaque. *Visual Neuroscience, 2*(2), 177–188.

Anderson, K. C., & Siegel, R. M. (1999). Optic flow selectivity in the anterior superior temporal polysensory area, STPa, of the behaving monkey. *Journal of Neuroscience, 19*(7), 2681–2692.

Ball, K., & Sekuler, R. (1979). Masking of motion by broadband and filtered directional noise. *Perception & Psychophysics, 26*(3), 206–214.

Ball, K., & Sekuler, R. (1987). Direction-specific improvement in motion discrimination. *Vision Research, 27*(6), 953–965.

Barton, J., Sharpe, J., & Raymond, J. (1996). Directional defects in pursuit and motion perception in humans with unilateral cerebral lesions. *Brain, 119*, 1535–1550.

Beardsley, S. A., & Vaina, L. M. (2001). A laterally interconnected neural architecture in MST accounts for psychophysical discrimination of complex motion patterns. *Journal of Computational Neuroscience, 10*(3), 255–280.

Beardsley, S. A., & Vaina, L. M. (2004a). A functional architecture for motion pattern processing in MSTd. In S. Thrun, L. Saul, & B. Schölkopf (Eds.). *Advances in neural information processing systems* (16, pp. 1451–1458). Cambridge, MA: MIT Press.

Beardsley, S. A., & Vaina, L. M. (2004b). Linking perception and neurophysiology for motion pattern processing: The computational power of inhibitory connections in cortex. In L. M. Vaina, S. A. Beardsley, & S. K. Rushton (Eds.). *Optic flow and beyond* (324, pp. 183–222). Dordrecht: Kluwer Academic Publishers.

Bevington, P. R. (1969). *Data reduction and error analysis for the physical sciences* (p. 336). New York: McGraw-Hill Book Company.

Bravo, M. J. (1998). A global process in motion segregation. *Vision Research, 38*(6), 853–863.

Britten, K. H., Shadlen, M. N., Newsome, W. T., & Movshon, J. A. (1993). Responses of neurons in macaque MT to stochastic motion signals. *Visual Neuroscience, 10*, 1157–1169.

Burr, D. C., Badcock, D. R., & Ross, J. (2001). Cardinal axes for radial and circular motion, revealed by summation and by masking. *Vision Research, 41*(4), 473–481.

Burr, D. C., Morrone, M. C., & Vaina, L. M. (1998). Large receptive fields for optic flow detection in humans. *Vision Research, 38*(12), 1731–1743.

Clifford, C. W. G., Beardsley, S. A., & Vaina, L. M. (1999). The perception and discrimination of speed in complex motion. *Vision Research, 39*(13), 2213–2227.

Coletta, N. J., Segu, P., & Tiana, C. L. (1993). An oblique effect in parafovial motion perception. *Vision Research, 33*(18), 2747–2756.

De Bruyn, B., & Orban, G. A. (1988). Human velocity and direction discrimination measured with random dot patterns. *Vision Research, 28*(12), 1323–1335.

Duffy, C. J., & Wurtz, R. H. (1991a). Sensitivity of MST neurons to optic flow stimuli. I. A continuum of response selectivity to large-field stimuli. *Journal of Neurophysiology, 65*(6), 1329–1345.

Duffy, C. J., & Wurtz, R. H. (1991b). Sensitivity of MST neurons to optic flow stimuli. II. Mechanisms of response selectivity revealed by small-field stimuli. *Journal of Neurophysiology, 65*(6), 1346–1359.

Duffy, C. J., & Wurtz, R. H. (1997). Medial superior temporal area neurons respond to speed patterns in optic flow. *Journal of Neuroscience, 17*(8), 2839–2851.

Edwards, M., & Badcock, D. R. (1993). Asymmetries in the sensitivity to motion in depth: a centripetal bias. *Perception, 22*, 1013–1023.

Freeman, T. C., & Harris, M. G. (1992). Human sensitivity to expanding and rotating motion: effects of complementary masking and directional structure. *Vision Research, 32*(1), 81–87.

Geesaman, B. J., & Andersen, R. A. (1996). The analysis of complex motion patterns by form/cue invariant MSTd neurons. *Journal of Neuroscience, 16*(15), 4716–4732.

Graziano, M. S., Anderson, R. A., & Snowden, R. J. (1994). Tuning of MST neurons to spiral motions. *Journal of Neuroscience, 14*(1), 54–67.

Greenlee, M. W. (2000). Human Cortical areas underlying the perception of optic flow: brain imaging studies. *International Review of Neurobiology, 44*, 269–292.

Gros, B. L., Blake, R., & Hiris, E. (1998). Anisotropies in visual motion perception: a fresh look. *Journal of Optical Society of America A—Optics Image Science and Vision, 15*(8), 2003–2011.

Lappe, M., & Duffy, C. J. (1999). Optic flow illusion and single neuron behavior reconciled by a population model. *European Journal of Neuroscience, 11*(7), 2323–2331.

Matthews, N., & Qian, N. (1999). Axis-of-motion affects direction discrimination, not speed discrimination. *Vision Research, 39*, 2205–2211.

Matthews, N., & Welch, L. (1997). Velocity-dependent improvements in single-dot direction discrimination. *Perception and Psychophysics, 59*(1), 60–72.

Meese, T. S., & Anderson, S. J. (2002). Spiral mechanisms are required to account for summation of complex motion components. *Vision Research, 42*(9), 1073–1080.

Meese, T. S., & Harris, M. G. (2001a). Broad direction bandwidths for complex motion mechanisms. *Vision Research, 41*(15), 1901–1914.

Meese, T. S., & Harris, M. G. (2001b). Independent detectors for expansion and rotation, and for orthogonal components of deformation. *Perception, 30*(10), 1189–1202.

Morrone, M. C., Burr, D. C., Di Pietro, S., & Stefanelli, M. A. (1999). Cardinal directions for visual optic flow. *Current Biology, 9*, 763–766.

Morrone, M. C., Burr, D. C., & Vaina, L. M. (1995). Two stages of visual processing for radial and circular motion. *Nature, 376*(6540), 507–509.

Morrone, M. C., Tosetti, M., Montanaro, D., Fiorentini, A., Cioni, G., & Burr, D. C. (2000). A cortical area that responds specifically to optic flow, revealed by fMRI. *Nature Neuroscience, 3*(12), 1322–1328.

Newsome, W. T., & Pare, E. B. (1986). MT lesions impair discrimination of direction in a stochastic motion display. *Society of Neuroscience Abstracts, 12*, 1183.

Perrone, J. A., & Stone, L. S. (1994). A model of self-motion estimation within primate extrastriate visual cortex. *Vision Research, 34*(21), 2917–2938.

Perrone, J. A., & Stone, L. S. (1998). Emulating the visual receptive-field properties of MST neurons with a template model of heading estimation. *Journal of Neuroscience, 18*(15), 5958–5975.

Raffi, M., & Siegel, R. M. (2004). Multiple cortical representations of optic flow processing. In L. M. Vaina, S. A. Beardsley, & S. K. Rushton (Eds.). *Optic flow and beyond* (324, pp. 3–22). Dordrecht: Kluwer Academic Publishers.

Raymond, J. E. (1994). Directional anisotropy of motion sensitivity across the visual field. *Vision Research, 34*(8), 1029–1039.

Read, H. L., & Siegel, R. M. (1997). Modulation of responses to optic flow in area 7a by retinotopic and oculomotor cues in monkey. *Cerebral Cortex, 7*(7), 647–661.

Rodriguez-Sanchez, A. J., Tsotsos, J. K., & Martinez-Trujillo, J. C. (2004). Velocity gradient information influences optical flow processing in human observers. *Journal of Vision, 4*(8), 606a.

Schaafsma, S. J., & Duysens, J. (1996). Neurons in the ventral intraparietal area of awake macaque monkey closely resemble neurons in the dorsal part of the medial superior temporal area in their responses to optic flow patterns. *Journal of Neurophysiology, 76*(6), 4056–4068.

Siegel, R. M., & Read, H. L. (1997). Analysis of optic flow in the monkey parietal area 7a. *Cerebral Cortex, 7*(4), 327–346.

Snowden, R. J., & Milne, A. B. (1996). The effects of adapting to complex motions: position invariance and tuning to spiral motions. *Journal of Cognitive Neuroscience, 8*(4), 412–429.

Snowden, R. J., & Milne, A. B. (1997). Phantom motion aftereffects–evidence of detectors for the analysis of optic flow. *Current Biology, 7*(10), 717–722.

Tanaka, K., Fukada, Y., & Saito, H.-A. (1989). Underlying mechanisms of the response specificity of expansion/contraction and rotation cells in the dorsal part of the medial superior temporal area of the macaque monkey. *Journal of Neurophysiology, 62*(3), 642–656.

Tanaka, K., & Saito, H. (1989). Analysis of motion of the visual field by direction, expansion/contraction, and rotation cells clustered in the dorsal part of the medial superior temporal area of the macaque monkey. *Journal of Neurophysiology, 62*(3), 626–641.

Te Pas, S. F., Kappers, A. M., & Koenderink, J. J. (1996). Detection of first-order structure in optic flow fields. *Vision Research, 36*(2), 259–270.

Tootell, R. B., Reppas, J. B., Kwong, K. K., Malach, R., Born, R. T., Brady, T. J., et al. (1995). Functional analysis of human MT and related visual cortical areas using magnetic resonance imaging. *Journal of Neuroscience, 15*(4), 3215–3230.

Vaina, L. M., Cowey, A., Eskew, R. T., LeMay, M., & Kemper, T. (2001). Regional cerebral correlates of global motion perception: evidence from unilateral cerebral brain damage. *Brain, 124*(Part 2), 310–321.

Vaina, L. M., & Soloviev, S. (2004). Functional neuroanatomy of heading perception in humans. In L. M. Vaina, S. A. Beardsley, & S. K. Rushton (Eds.). *Optic flow and beyond* (324, pp. 109–138). Dordrecht: Kluwer Academic Publishers.

Vaina, L. M., Solovyev, S., Kopcik, M., & Chowdhury, S. (2000). Impaired self-motion perception from optic flow: a psychophysical and fMRI study of a patient with a left occipital lobe lesion. *Society of Neuroscience Abstracts, 26*, 1065.

Watamaniuk, S. N. J., Sekuler, R., & Williams, D. W. (1989). Direction perception in complex dynamic displays: the integration of direction information. *Vision Research, 29*(1), 47–59.

Zemel, R. S., & Sejnowski, T. J. (1998). A model for encoding multiple object motions and self-motion in area MST of primate visual cortex. *Journal of Neuroscience, 18*(1), 531–547.

Zhao, L., Vaina, L. M., LeMay, M., Kader, B., Chou, I. S., & Kemper, T. (1995). Are there specific anatomical correlates of global motion perception in the human visual cortex? *Investigative Ophthalmology & Visual Science, 36*(4), S56.